Sensors & Transducers, Vol. 193, Issue 10, October 2015, pp. 145-153

Sensors & Transducers

http://www.sensorsportal.com

Improving Systems Dynamics by Means of Advanced Signal Processing – Mathematical, Laboratorial and Clinical Evaluation of Propofol Monitoring in Breathing Gas

[1, 2] Dammon ZIAIAN, [2, 3] Philipp ROSTALSKI, [4] Astrid Ellen BERGGREEN, [4] Sebastian BRANDT, [4, 5] Martin GROSSHERR, [4] Hartmut GEHRING, [2, 6] Andreas HENGSTENBERG and [1] Stefan ZIMMERMANN

[1] Institute of Electrical Engineering and Measurement Technology, Appelstraße 9a, 30167 Hannover, Germany
Tel.: +49 511 762 4671,
[2] Research Unit, Draegerwerk AG & Co.KGaA, Moislinger Allee 53-55, 23558 Luebeck, Germany
[3] Now at Universitaet zu Luebeck, Institut fuer Medizinische Elektrotechnik, Ratzeburger Allee 160, 23562 Luebeck, Germany
Tel.: +49 451 3101 6200,
[4] University of Luebeck, Dept. of Anesthesiology and Intensive Care Medicine, Ratzeburger Allee 160, 23538 Luebeck, Germany
Tel.: +49 451 500 4057,
[5] Segeberger Kliniken, Abteilung für Kardioanästhesie,Am Kurpark 1, 23795 Bad Segeberg, Germany
Tel.: +49 451 593 608
[6] Now at SICK AG, Merkurring 20, 22143 Hamburg, Germany
E-mail: dammon.ziaian@web.de, zimmermann@geml.uni-hannover.de, rostalski@ime.uni-luebeck.de, E-mail: berggreen@anaesthesie.uni-luebeck.de, sebastian.brandt@uksh.de, hartmut.gehring@uni-luebeck.de, martin_grossherr@hotmail.com, andreas.hengstenberg@online.de

Received: 31 August 2015 /Accepted: 5 October 2015 /Published: 30 October 2015

Abstract: Electrochemical sensors are used in various gas measurement applications and are available for different gases. Depending on the application, the sensor might need to be installed far away from the actual measurement site, requiring the use of long sampling lines. Examples are portable gas measurement devices in which remote locations like tanks and chemical reactors need to be monitored. But also medical applications, where the sensors cannot be positioned in close vicinity to the patient, are common like, e.g., the side-stream measurement of breathing gas. Due to the characteristics of electrochemical sensors and to the adsorption and desorption behavior of sampling lines for different gases, the electrical sensor signal may indicate long response times. In this paper, we propose an on-line signal processing algorithm which is capable to significantly improve the performance. After characterizing the dynamic behavior of the sensor system, a properly designed deconvolution filter is used to reduce response time and signal noise. Within this article, we also provide an

example of this algorithm for a novel electrochemical sensor for the measurement of the anesthetic agent propofol in exhaled air. For this application, the acceleration is prerequisite for the measurement chain to be of practical use in a clinical setting. Our goals, to establish measurement dynamics to record the physiologic parameter and to reduce non-physiological disturbances, were achieved with additional reserves. This article is based on [1] and is extended by original clinical data. As an example, we present propofol monitoring in breath of one patient in order to demonstrate the performance of the introduced algorithm in a real clinical application. We proved that the electrochemical sensor, associated with the provided algorithm, is capable for real-time monitoring in a clinical setting.

Keywords: Deconvolution, Electrochemical sensor, Propofol, Response time, Noise reduction.

1. Introduction

Electrochemical sensors [2] are widely used for measuring gases in various industries, most notably process industry, oil and gas, but also in medical applications. Various research and development activities have gone into optimizing the design, material and electrochemical properties of this type of gas sensor in order to improve response time, selectivity, accuracy, precision, minimizing the drift and other adverse effects. However, a certain delay in the response due to the diffusion, chemical reaction but also adsorption/desorption is inherent in any sensor.

We will discuss a specific medical application for an electrochemical gas sensor, but similar techniques may be used in other areas. After describing the specific application and measurement chain for the physiological signal considered for the remainder of this article, we will discuss the design of a deconvolution filter to accelerate the system response while filtering non-physiological disturbances. The performance of the filter is derived mathematically and analyzed, both based on laboratory measurements and in a clinical setting. The intention of this work is to assess how far the usage of this electrochemical sensor for patients is feasible under real clinical conditions. For that reason breathing gas was sampled of a number of patients which received propofol for anesthesia and analyzed online. In Section 2, the specific application and the experimental setup are described. Furthermore, mathematical explanations on modeling and the design of the algorithm are given and the clinical setup for data collection at the bed side is introduced. Results of the signal acceleration and noise reduction are presented in Section 3 together with breath measurements of one patient during the awakening phase of anesthesia. At the end, the application of advanced signal processing is discussed and concluded in Section 4.

2. Material and Methods

2.1 Specific Application

As a practically relevant example, an electro-chemical gas sensor which is used to quantify the concentration of 2,6-Diisopropylphenol, also known as propofol, is considered [3]. Propofol is applied as an anesthetic agent for humans and animals. It is intravenously administered in the formulation of a lipid emulsion. Its volatile characteristics allow detecting propofol in the breathing gas after injection [4]. During anesthesia the exhaled concentration appears in the order of around 20 ppb (parts per billion) [5, 6]. As a result, the required sensitivity and accuracy of the sensor need to be suitable to ensure a reliable measurement.

When handling substances in such low concentrations, effects of adsorption and desorption along the measurement chain have a particularly strong impact. In the case discussed here, the carrier gas is drawn through a 2.5 m long sampling line from the propofol source which happened to be a gas cylinder (carrier gas: N2, propofol concentration: 40 ppb ±30 % rel. standard deviation). Since the true concentration of one cylinder lies between 28 ppb and 52 ppb according to the vendor, the sensitivity of the sensor cannot be stated based on the actual data. The schematic of the setup is presented in Fig. 1. A sampling flow of 180 ml/min is generated with the help of a pump. Hence, the carrier gas is led through the sampling line to interact with the sensor.

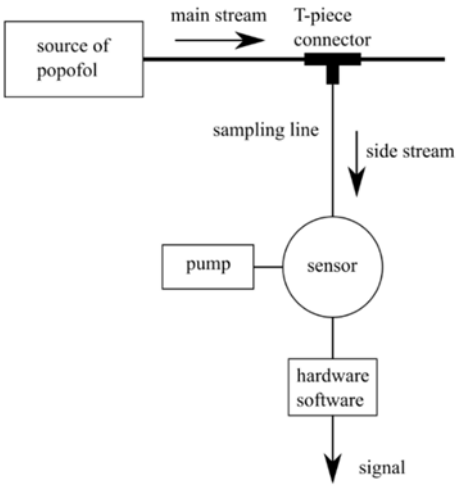

Fig. 1. Schematic of the experimental setup. The side stream is driven through the sampling line to pass the electrochemical sensor for detection. A T-piece connector is used for switching.

The saturation of propofol on the inner surface of the line leads to a major dynamic delay in time before the electrochemical sensor is able to detect the absolute concentration. Besides the delay caused by the sampling system, the response characteristics of the electrochemical sensor itself adds further major delay. It is assumed that these two effects are responsible for the main delay. Another cause refers to the volume of the line which the gas has to pass before reaching the sensor. This volume leads to a constant, non-dynamic delay. Considering an inner tubing diameter of 3.2 mm, given flow rate and given length of the sampling line, a dead time of 5.4 sec is created. However, 5.4 sec are negligible in contrast to the major dynamic delay reasons.

Recorded signals are usually corrupted by noise. Owing to the pump, to thermal noise within the electronic components and other effects, all measured values possess a specific variance. Besides the minimization of the response time, another objective of the signal processing algorithm proposed in this article is to increase signal quality in real-time. We have been aware of the fact that signal acceleration might lead to over-proportional amplification of non-physiological disturbances. In the light of the aforesaid, it is mandatory to seek for this goal.

2.2. System Identification

Any signal processing procedure needs to be tailored to the specific application. This can be either done heuristically by following tuning rules or by using a model-based procedure. In this publication we follow the latter route. System identification is the necessary first step to identify the underlying system model.

2.2.1. Recording the Step Response

A step change of propofol gas was applied in order to excite the measurement system. Data was recorded using the setup illustrated in Fig. 1. At defined times the propofol-free sampling line was connected and disconnected to the main stream which contained propofol saturated gas of approximately 40 ppb. One standardized cycle consists of three minutes of recording the baseline with propofol-free room air, followed by 30 minutes of connection to the main stream. And finally, the system was purged for 30 minutes with room air by disconnection from the T-piece connector. In Fig. 2, the input excitation is shown in green and the resulting step response of the sensor system in blue. Dotted lines indicate the 90 % value and the steady state of the response. In this particular measurement it lasts

$$t_{90} = 401\,\text{sec} \tag{1}$$

before 90 % of the steady state value is reached.

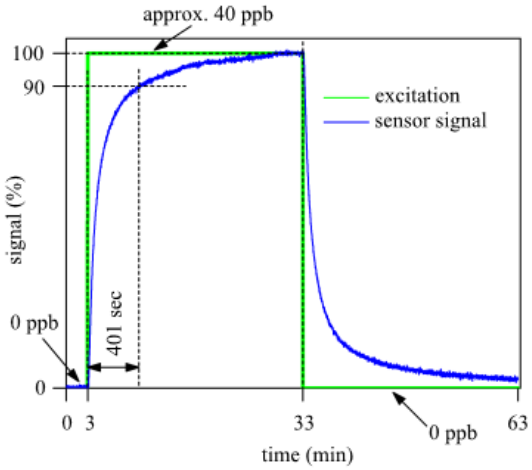

Fig. 2. Result of one measurement cycle. Excitation sequence is shown in green and sensor signal in blue. 90 % of the ultimate value is reached within 401 sec after connecting to the main stream.

To quantify the precision of each measurement the signal to noise ratio (SNR), here defined as

$$SNR = \frac{\text{amplitude}}{\text{standard deviation}} \tag{2}$$

is calculated. The amplitude derives from the mean value of a short time period towards the end of exposure to propofol gas and is thus equal to the steady state value. The SNR may be understood as an intra-measurement precision, whereas the evaluation of a set of multiple measurements leads to the overall precision of the sensor system. A higher SNR reflects a better precision. For the measurement shown in Fig. 2 the resulting ratio appears as 367, indicating a rather low noise situation. Again, the actual noise situation is not the reason for seeking a better SNR, but the signal acceleration, explained in what follows, makes it mandatory.

2.2.2. Modeling and Parameter Identification

System identification can be done using different methods, ranging from white box modeling based on first-principles with parameters derived using physically measures to black box modeling, where no prior knowledge about the model is available. We will follow the latter approach with two assumptions on the model structure. The step response from Fig. 2 suggests a first or second order response, without overshoot and no oscillatory components. A reasonable model structure (second order) in the time domain is thus given by

$$f_{\text{mod}\,el}(t) = k\left(1 + e^{-\frac{t}{T_1}}\frac{T_z - T_1}{T_1 - T_2} + e^{-\frac{t}{T_2}}\frac{T_z - T_2}{T_2 - T_1}\right). \tag{3}$$

Therein k represents the static gain. T_1, T_2 and T_z characterize the dynamics of the system and t is set to be the time variable. By means of the Laplace transformation [7] the same relationship may be stated in the frequency domain as

$$f_{model}(t) \Leftrightarrow F_{model}(s) \tag{4}$$

$$F_{model}(s) = k\frac{T_z}{T_1 T_2}\frac{s+\frac{1}{T_z}}{(s+\frac{1}{T_1})(s+\frac{1}{T_2})} \tag{5}$$

$$= k\frac{T_z s+1}{(T_1 s+1)(T_2 s+1)}, \tag{6}$$

where s is defined as the complex angular frequency.

The parameters of this model are computed using an optimized fitting procedure. With the help of a least squares method the set of parameters k, T_z, T_1 and T_2 are determined which yield the smallest sum of squares error between the modeled and the actual response. The best values found for this particular setup are as follows:

$$k = 1 \tag{7}$$

$$T_z = 413.03 \text{ sec} \tag{8}$$

$$T_1 = 536.95 \text{sec} \tag{9}$$

$$T_2 = 52.49 \text{ sec} \tag{10}$$

In Fig. 3 the result of the modeling and parameter identification is illustrated.

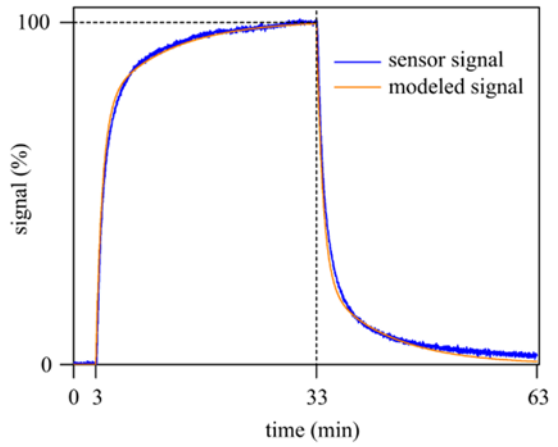

Fig. 3. Result of the modeling and parameter identification. The measured time course is displayed in blue and the modeled signal in orange.

The blue line represents the measurement as displayed in Fig. 2. After finding an appropriate model structure and reasonable parameters the modeled signal, drawn in orange, can be calculated. The visual matching indicates that the fitted curve agrees well with the measurement. The remaining mismatch is likely to be a result of the inherent non-linearity of different dynamics for rising and falling concentrations. With a hybrid model including two switching dynamics for rising and falling signal response respectively the fitting curve would show a better match, albeit at the price of mathematical complexity and a non-linear behavior.

2.3. Design of Algorithm

In [8], the physiological lung dynamics regarding the propofol exchange from blood plasma to breathing gas are described by a first order differential equation. Its time constant T, which is defined as the time to reach 63 % of the final propofol concentration in the lung due to a sudden change in the blood plasma propofol level, is estimated using clinical patient data to be $T = 414\text{sec}$ in mean, approximately corresponding to a respond time of $t_{90,breath} = 952$ sec. We expect that a proper metering for anesthesia monitoring is performed when the detection happens three times faster than the parameter might change. Considering this, the sensing system should not exceed a maximal response time of $t_{90,\max} = 317$ sec for a clinically relevant measurement of propofol in breath.

As mentioned before, the main issue of the electrochemical measurement system for propofol is its long response time. Major causes for this are adsorption/desorption effects in the sampling system as well as the inherent measurement dynamics of the electrochemical sensor itself. All of these elements lead to a delayed response between the propofol concentration in breath and the signal provided by the sensor with a typical response time of $t_{90} = 401\text{sec}$. Fortunately in a clinical environment most of the factors determining the delay are almost constant over time and depend only on the measurement chain. The delay can thus be compensated by using linear signal processing. The design of such an algorithm is the content of this section.

2.3.1. Deconvolution

The measured signals $\phi(t)$ are the result of the time course of the propofol concentration in the breathing gas $c_{breath}(t)$ and $f_{system}(t)$, which is meant to be the unknown response characteristic of the measuring system,

$$\phi(t) = f_{system}(t) * c_{breath}(t), \tag{11}$$

where $*$ denotes the convolution operator.

During a measurement, $f_{model}(t)$ (identified in Section 2.2.2) and all past values of $\phi(t)$ are known. The aim is to compute the original source signal $c_{breath}(t)$ with these known information. It is possible to estimate the delayed signal by inverting the slow dynamic components of the measurement chain. Mathematically, this means that we need to invert the effect of the convolution through deconvolution with all transfer elements between source and electrical signal of the sensor. Deconvolution is best understood in frequency domain. Each frequency component is delayed and damped individually by the measurement chain

$$\Phi(s) = F_{system}(s) C_{breath}(s). \quad (12)$$

The idea of deconvolution is simply to shift and amplify each frequency component accordingly to reverse this effect. Based on the model identified in Section 2.2.2, we can approximate $C_{breath}(s)$ through deconvolution as

$$\hat{C}_{breath}(s) = \Phi(s) \cdot \mathrm{inv}\left(F_{model}(\mathrm{s})\right) \quad (13)$$

$$= F_{system}(s) C_{breath}(s) \frac{1}{F_{model}(\mathrm{s})}, \quad (14)$$

where $\Phi(s)$ denotes the frequency transform of the measured signal, $F_{model}(\mathrm{s})$ is the model identified in the previous section and $\hat{C}_{breath}(s)$ provides the estimated propofol concentration.

This procedure, however, is not realizable for a number of reasons in practical setting requiring real-time computation in a medical device. First and foremost, the deconvolution equation (14) as given above cannot be realized, at least not without modification. Any causal system satisfies the property that its numerator order is equal or lower than its denominator order. This translates into the fact that at each point in time we only measure the next signal value but not its time derivatives.

$$\mathrm{inv}\left(F_{model}(\mathrm{s})\right) = \frac{1}{F_{model}(\mathrm{s})} = \frac{(T_1 s + 1)(T_2 s + 1)}{k(T_z s + 1)} \quad (15)$$

Not keeping causality would incorrectly imply that an effect may appear before its cause.

Another potential issue of a simple inversion is noise. In reality, (12) can be rewritten as

$$\Phi(s) = F_{system}(s) C_{breath}(s) + R(s), \quad (16)$$

where $R(s)$ denotes the Laplace transform of the noise. The estimation of $\hat{C}_{breath}(s)$ considering the noise term results in

$$\hat{C}_{breath}(s) = \frac{F_{system}(s) C_{breath}(s)}{F_{model}(\mathrm{s})} + \frac{R(s)}{F_{model}(\mathrm{s})}. \quad (17)$$

Most real systems, including the measurement chain in question, have a low-pass behavior which dampens high frequency noise. Inverting the transfer function of such a system would result in a high-pass behavior which highly amplifies non-physiological signal components such as noise and distorts the actual propofol signal. Our aim, to increase the SNR, addresses this over-proportional amplification of noise during deconvolution.

2.3.2. Causality and Noise Treatment

One potential solution to overcome the issues mentioned above is to augment the deconvolution filter in (17) by a low-pass filter

$$\underbrace{\hat{C}_{breath}(s)}_{\text{estimation}} = F_{system}(s) C_{breath}(s) \frac{F_{filter}(s)}{F_{model}(\mathrm{s})} + R(s) \frac{F_{filter}(s)}{F_{model}(\mathrm{s})} \quad (18)$$

$$= \left(F_{system}(s) C_{breath}(s) + R(s)\right) \frac{F_{filter}(s)}{F_{model}(\mathrm{s})} \quad (19)$$

$$= \underbrace{\Phi(s)}_{\text{measurement}} \underbrace{\frac{F_{filter}(s)}{F_{model}(\mathrm{s})}}_{\text{algorithm}}. \quad (20)$$

If the filter order is chosen high enough, the causality of the overall system is satisfied. Since $\mathrm{inv}\left(F_{model}(\mathrm{s})\right)$, see equation (15), has a numerator order of two and a denominator order of one, a low-pass filter $F_{filter}(s)$ with an order of at least one would therefore fulfill the need for causality.

2.3.3. Low-pass Filter

Dedicated to the electrochemical measurement system and to the application requirements the following low-pass filter –a second order Butterworth filter [9] – has shown sufficient performance. Its flatness and linearity in the pass band and the uncomplicated design are beneficial in our case. Other types of filtering may be more favorable depending on the application.

In order to determine a suitable cut-off frequency we considered the appearing dynamics. The dynamics of propofol exhalation in breathing gas can be derived from [8, 10]. In a subsequent adjustment procedure our filter parameters have been fine-tuned during application to obtain a satisfying compromise between

noise rejection and response time. With the resulting cut-off angular frequency of

$$\omega = 2\pi f = 4 \cdot 10^{-2} \frac{\text{rad}}{\text{sec}} \tag{21}$$

the transfer function of the Butterworth filter is given as

$$F_{filter}(s) = \frac{0.0016 \frac{\text{rad}^2}{\text{sec}^2}}{\text{s}^2 + 0.05657 s \frac{\text{rad}}{\text{sec}} + 0.0016 \frac{\text{rad}^2}{\text{sec}^2}}. \tag{22}$$

2.3.4. The Resulting Algorithm and its Software Implementation

As implied in (20), the algorithm for the signal processing is composed as

$$F_{algorithm}(\text{s}) = \frac{F_{filter}(s)}{F_{model}(\text{s})}. \tag{23}$$

For our particular case, the algorithm results in

$$F_{algorithm}(\text{s}) = \frac{(T_1 s + 1)(T_2 s + 1)}{k(T_z s + 1)} \cdot \frac{0.0016 \frac{\text{rad}^2}{\text{sec}^2}}{\text{s}^2 + 0.05657 s \frac{\text{rad}}{\text{sec}} + 0.0016 \frac{\text{rad}^2}{\text{sec}^2}} \tag{24}$$

due to the model characterized in Section 2.2.2 and due to the filter described in Section 2.3.3. All poles of $F_{algorithm}(s)$ are negative, thus stability is ensured. The continuous frequency domain is helpful for design matters. But for the implementation as a real-time capable algorithm few more steps are required. Since the sensors output is available digitally it exists of discrete values appearing in a specific rate. Therefore, it is necessary to transform into the discrete time domain. With the use of the bilinear transform [11] and the properties of the z-transform [12] the algorithms output at a certain point in time can be stated as a sum. (25) depicts a general description. Therein, $y(\text{k})$ expresses the algorithms output and $x(\text{k})$ the measured value, while k denotes the discrete time variable.

$$y(\text{k}) = \frac{1}{a_0}\left[b_0 x(\text{k}) + b_1 x(\text{k}-1) + \cdots + b_n x(\text{k}-\text{n}) - a_1 y(\text{k}-1) + \cdots + a_n y(\text{k}-\text{n})\right] \tag{25}$$

Hence, $y(\text{k})$ is calculated as a linear combination of previous calculations and measurements, whereas $a_{0\ldots\text{n}}$ and $b_{0\ldots\text{n}}$ denote the coefficients characterizing the algorithm.

Applied on $F_{algorithm}(s)$ of (24), we find a compact description to be implemented in any software as a real-time capable signal processing algorithm:

$$y(\text{k}) = \frac{1}{a_0}\left[b_0 x(\text{k}) + b_1 x(\text{k}-1) + b_2 x(\text{k}-2) + b_3 x(\text{k}-3) - a_1 y(\text{k}-1) - a_2 y(\text{k}-2) + a_3 y(\text{k}-3)\right] \tag{26}$$

After transformation for a sampling rate of 1 Hz the coefficients can be found in Table 1. The given precisions of decimal places are required for stability, when the algorithm is programmed to perform.

Table 1. Discrete Time Coefficients for a 1 Hz-Clocked Deconvolution Filter.

Coefficient	Value
a_0	1
a_1	-2.9551616730526264
a_2	2.9113070363222864
a_3	-0.95614323255658584
b_0	0
b_1	0.060676477761667597
b_2	-0.12009490846751848
b_3	0.059420561418924996

2.4. Clinical Data

As clinical patient data are part of our evaluations, we will give an overview of how this data was collected.

With written informed consent and approval of the local ethnic committee patients undergoing surgeries demanding anesthesia were monitored. Anesthesia was performed using propofol and remifentanil. Their application was performed by means of target controlled infusion pumps. During a standardized course of anesthesia, breathing gas was sampled in order to quantify the propofol concentration in real-time. Standardly, the blood plasma target concentration was maintained at 2 µg/ml for 15 min before the intake of propofol and remifentanil were stopped. This phase took place after the actual surgical procedure. The connection to the ventilation circuit for the propofol measurement happened postoperatively. In Fig. 4, the clinical setup is referred to. While similarity to the laboratorial setup is given, the main difference regards the T-piece connector which is placed between the patient and the ventilator machine. The quantification of the propofol concentration occurred in real-time using the technologies explained in the previous sections.

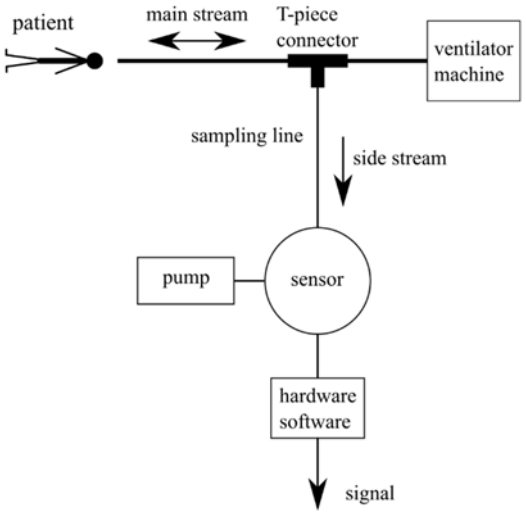

Fig. 4. Clinical setup for the measurement of propofol in breathing gas of a ventilated patient.

3. Results

Due to the concise description of the algorithm presented in the previous section it is possible to calculate an accelerated signal in real-time as well as retrospectively. Further on, results are presented for a step change of the propofol concentration as displayed in Fig. 2 of Section 2.2.2 and for repeated measurements.

In Fig. 5, the post-processed signal is illustrated in red. This example visualizes the improvement possible through signal processing. In this particular case, the response time t_{90} is notably reduced from 401 seconds to 104 seconds. In Section 2.3, the maximal tolerated response time is mentioned to be $t_{90,\max} = 317\text{sec}$. Therefore, this requirement is fulfilled with an additional reserve. The secondary objective stated is an increase of precision. By noise treatment consideration during the filter design the SNR is enhanced from 367 to remarkably 1482. As the measuring system is afflicted with non-linearity the algorithm shows a different result for rising and falling signals. Both overshooting and undershooting lead to higher (102.3 %) and lower (-1.1 %) values. However, the error stays below ±5 %, which is an acceptable result compared to the enhancements in response time and noise reduction.

To express the performance and the repeatability of the algorithm, repeated measurements were evaluated. The same setup was used at different times whereas the algorithm was executed online in real-time. As an example, the results for three repetitions are displayed in Fig. 6. Pairwise-colored curves denote sensor signals and their related real-time processed estimation of the input excitation. It might be that a drift of the propofol source concentration or of the sensor sensitivity have occurred during the repetitions. Even though, the algorithm has performed stable and with expected results. Summarized, we observe that results are highly reproducible and that the algorithm performs similarly in real-time as long as main parameters of the system do not significantly change and linearity is given for the tolerated concentration range. This result is valid for the discussed clinical practice and also for several other applications of electrochemical and other sensors.

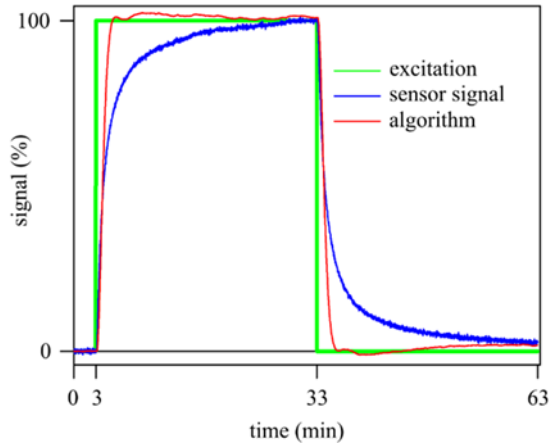

Fig. 5. The result of the signal post-processing is displayed in red, the sensor signal used for the calculation in blue.

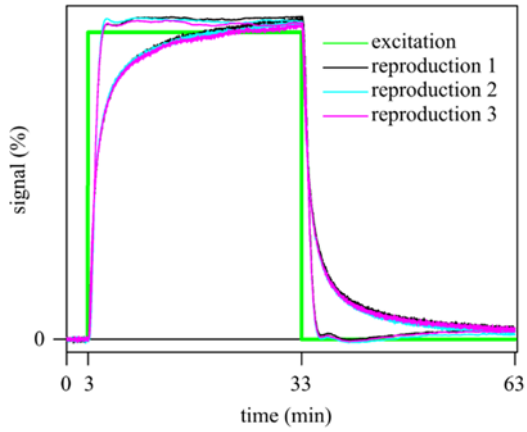

Fig. 6. Three reproduced measurements 1- 3 are illustrated to express the repeatability. The algorithm was applied in real-time during each measurement. Pairs of the same color represent related sensor and algorithm signals.

In addition to mathematical and laboratorial considerations, we present the performance of the algorithm in a field application while measuring the exhaled propofol concentration of a narcotized patient. In Fig. 7, the time series of the raw sensor signal together with the output of the algorithm are illustrated. The sampling line of the sensor module was connected to the main circulatory ventilation right after the plasma target concentration was set to 2 µg/ml. About 15min later, the target was set to 0 µg/ml leading to an instant stop of infusion. As soon as the intubated patient woke up, the sampling line was disconnected from the respiratory circuit.

Consequently, room air was sampled hereafter. During that phase, it is possible to visually recognize that the use of the algorithm leads to an accelerated signal when connecting and disconnecting the sampling line. It performed stable and the noise level was reduced as expected.

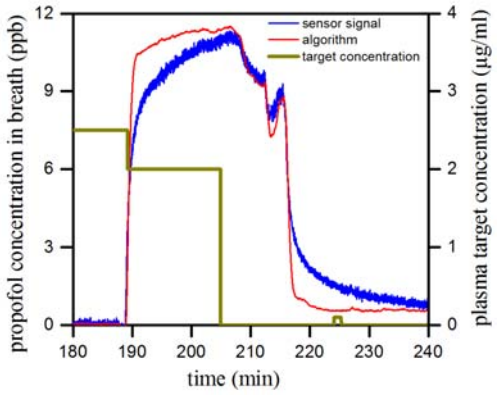

Fig. 7. Schematic of the experimental setup. The side stream is driven through the sampling line to pass the electrochemical sensor for detection. A T-piece connector is used for switching.

4. Discussion and Conclusion

In various practical applications of electrochemical sensors a sampling line is required to transport the gas from the sampling site to the sensor. This together with the dynamics of the sensor itself might lead to significant delays and adverse measurement dynamics, rendering the electrochemical measurement signal useless for the application. To overcome this obstacle, a solution in form of an accelerating algorithm is presented.

In this article, we have demonstrated that the application of advanced signal processing can help to optimize the performance of electrochemical measurement systems with long sampling lines. For the example of an electrochemical propofol sensor, the response time could significantly be reduced by a factor of 9.2 while the SNR could be increased at the same time by a factor of 4. Furthermore, the proposed procedure involves only straight forward model-based design steps and should thus easily be transferable to other applications. Starting with a modeling and system identification step, the characteristics of the sensor system are identified. Here, a second order equation is used to model the sensor response. Noise considerations lead to the specification of a second order low-pass Butterworth filter and to the design of a deconvolution algorithm.

Our primary objective has been to realize a detecting system able to observe the propofol concentration in patients' exhaled breath at least three times faster than this physiological parameter might change. With the help of the presented algorithm the accelerated response time of $t_{90} = 104\,\text{sec}$ is 9.2 times faster than the patients average breath propofol concentration change with $t_{90,breath} = 952\,\text{sec}$.

The patient with the fastest exhalation dynamic observed in [8] does have a time constant of $T = 227\,\text{sec}$. This implies a maximal permitted response time of $t_{90,\max} = 174\,\text{sec}$ for the measuring device. Thus, using the presented acceleration algorithm the propofol sensors system is even suitable to monitor such, probably exceptional, fast exhalation dynamics.

Another issue discussed in the paper relates to noise. On the one hand more accurate signals are advantageous in general and on the other hand we are aware of the fact that deconvolution might lead to exceedingly higher noise levels. With a proper choice of a low-pass filter, this effect could be coped with, resulting in a significantly improved SNR, albeit the SNR has been acceptable before processing.

With the decision to run measurements in a real clinical environment, we have achieved insights for propofol monitoring in clinical practice. First of all, we showed that an electrochemical sensor is capable to quantify the propofol concentration in breathing gas in real-time and with an acceptable response time. So far, clinical circumstances have been a significant obstacle leading to large response times in all practical settings. Additionally the interaction with the ventilator machine, disposable articles and clinical air, for example, were questionable. As a result of our study, we observed a stable, accelerating and noise reducing performance of the algorithm following the predictions of our laboratory measurements.

One difference to a clinical setup is regarded to the relative humidity conditions of the gas, which appear much higher when patients' breathing gas is sampled. Influences of humidity were not observable during other investigation. Thus, the impact is not part of this work and might be a topic to address in future.

It is worth mentioning that the application of the presented signal processing is not limited to the clinical setting. Especially, portable gas detection devices are often used in conjunction with long samplings reaching up to 30 m and thus leading to remarkable delays beside the dead time delays due to volume.

Technologically, other more advanced signal processing algorithms come to mind such as Wiener Filter [13], (linear/nonlinear) Kalman Filter [14] or moving horizon estimation, however at a price of a higher complexity. It will be part of ongoing research activities to evaluate these techniques in the context of electrochemical sensors with long sampling lines and to compare the results against the surprisingly simple and effective solution provided here.

References

[1]. D. Ziaian, P. Rostalski, A. Hengstenberg and S. Zimmermann, Reducing System Response Time and Noise of Electrochemical Gas Sensors - Discussed

for Propofol Monitoring in Breathing Gas, in *Proceedings of the 6th International Conference on Sensor Device Technologies and Applications* (*SENSORDEVICES'15)*, Venice, Italy, August 23 - 28, 2015, pp. 85–90.

[2]. P. J. Gellings and H. J. Bouwmeester, The CRC Handbook of Solid State Electrochemistry, Chapter 10, *CRC Press*, 1997.

[3]. Package leaflet: Information for the user Diprivan 10 mg/ml (1 %) Emulsion for Injection or Infusion, 2015, URL: https://www.medicines.org.uk/emc/medicine/8375 [accessed: 2015-06-19].

[4]. M. Grossherr, A. Hengstenberg, T. Meier, L. Dibbelt, K. Gerlach, and H. Gehring. Discontinuous Monitoring of Propofol Concentrations in Expired Alveolar Gas and in Arterial and Venous Plasma during Artificial Ventilation, *Anesthesiology*, Vol. 104, 2006, pp. 786–790.

[5]. M. Grossherr et al. Propofol concentration in exhaled air and arterial plasma in mechanically ventilated patients undergoing cardiac surgery, *British Journal of Anesthesia*, Vol. 102, No. 5, 2009, pp. 608–613.

[6]. A. Taketa, K. Masui, and T. Kalama, On-line Monitoring of End-tidal Propofol Concentration in Anesthetized Patients, *Anesthesiology*, Vol. 106, pp. 659–664, 2007.

[7]. H. Dwyer, The Laplace Transform: Motivating the Definition, *CODEE Journal*, Vol. 125, pp. 1231–1238, 2011, URL: http://www.codee.org/ref/CJ11-0116 [accessed: 2015-06-19].

[8]. D. Ziaian et al., Pharmacokinetic modeling of the transition of propofol from blood plasma to breathing gas, in *Proceedings of the IEEE International Symposium on Medical Measurements and Applications (MeMeA'14)*, Lisboan, Portugal, June 11-12, 2014, pp. 80–84.

[9]. D. Gordon, E. Robertson, and J. J. Dowling, Design and responses of Butterworth and critically damped digital filters, *Journal of Electromyography and Kinesiology*, Vol. 13, 2003, pp. 569–573.

[10]. C. Horns, D. Wieck, S. Prawn, M. Dolce, C. Patel, and G. Schelling, Time course of expiratory propofol after bolus injection as measured by ion molecule reaction mass spectrometry, *Analytical and Bioanalytical Chemistry*, Vol. 403, No. 2, April 2012, pp. 555–561.

[11]. G. Zhang, X. Chen, and T. Chen, Digital redesign via the generalized bilinear transformation, *International Journal of Control*, Vol. 82, No. 4, April 2009, pp. 741–754.

[12]. J. R. Magazine and L. A. Zadie, The analysis of sampled-data systems, *Transactions of the American Institute of Electrical Engineers, Part II: Applications and Industry*, Vol. 71, No. 5, Nov 1952, pp. 225–234.

[13]. N. Wiener, Extrapolation, Interpolation, and Smoothing of Stationary Time Series, *Wiley*, New York, 1949.

[14]. R. E. Kalman, A New Approach to Linear Filtering and Prediction Problems, *Journal of Fluids Engineering*, Vol. 82, No. 1, March 01 1960, pp. 35–45.